Catchment drainage network scaling laws found experimentally in overland flow morphologies

Citation for published version:
Cheraghi, M, Rinaldo, A, Sander, G, Perona, P & Barry, A 2018, 'Catchment drainage network scaling laws found experimentally in overland flow morphologies', *Geophysical Research Letters*.
https://doi.org/10.1029/2018GL078351

Digital Object Identifier (DOI):
10.1029/2018GL078351

Published In:
Geophysical Research Letters

Catchment drainage network scaling laws found experimentally in overland flow morphologies

Mohsen Cheraghi[1*], Andrea Rinaldo[2,3], Graham C. Sander[4], Paolo Perona[5], D. A. Barry[1]

[1]Ecological Engineering Laboratory (ECOL), Institute of Environmental Engineering (IIE), School of Architecture, Civil and Environmental Engineering (ENAC), École Polytechnique Fédérale de Lausanne (EPFL), Lausanne, Switzerland

[2]Ecohydrology Laboratory (ECHO), Institute of Environmental Engineering (IIE), School of Architecture, Civil and Environmental Engineering (ENAC), École Polytechnique Fédérale de Lausanne (EPFL), Lausanne, Switzerland

[3]Dipartimento di Ingegneria Civile Edile e Ambientale, Universitá di Padova, Padua, Italy

[4]School of Architecture, Civil and Building Engineering, Loughborough University, Loughborough, UK

[5]School of Engineering, Institute for Infrastructure and Environment, The University of Edinburgh, Edinburgh, UK

*To whom correspondence should be addressed

Key Points:

- Unchanneled surface under spatially non-uniform rainfall shows the same scaling structures as catchment
- The power law exponents remain constant during the surface evolution

Corresponding author: M. Cheraghi, `mohsen.cheraghi@epfl.ch`

Abstract

The scaling relation between the drainage area and stream length (Hack's law), along with exceedance probabilities of drainage area, discharge and upstream flow network length are well known for channelized fluvial regions. We report here on a laboratory experiment on an eroding unconsolidated sediment for which no channeling occurred. Laser scanning was used to capture the morphological evolution of the sediment. High intensity, spatially non-uniform rainfall ensured that the morphology changed substantially over the 16-h experiment. Based on the surface scans and precipitation distribution, overland flow was estimated with the D8 algorithm, which outputs a flow network that was analyzed statistically. The abovementioned scaling and exceedance probability relationships for this overland flow network are the same as those found for large scale catchments and for laboratory experiments with observable channels. In addition, the scaling laws were temporally invariant, even though the network dynamically changed over the course of experiment.

1 Introduction

Even with markedly different environmental and geological conditions, catchment drainage networks have similar geometrical characteristics that take the form of power laws [*Rodríguez-Iturbe and Rinaldo*, 1997; *Rinaldo et al.*, 2014], as measured for different areas [*Hack*, 1957; *Mandelbrot*, 1977; *Tarboton et al.*, 1989; *Rigon et al.*, 1996]. Hack's law [*Hack*, 1957] states that the upstream length (l, the longest flow path into each point) and drainage area (A) are related via a power law scaling ($l = A^h$) where the exponent h (Hack exponent) was measured in the range of [0.5-0.7] for different river networks [*Hack*, 1957; *Gray*, 1961; *Mueller*, 1972; *Mosley and Parker*, 1973; *Montgomery and Dietrich*, 1992; *Maritan et al.*, 1996; *Rigon et al.*, 1996, 1998], with an average value of about 0.58 [*Willemin*, 2000]. Also, for the fluvial parts of landscapes, power-law relations with exponent ranges of [0.42-0.45] and [0.5-0.9] were observed for the exceedance probabilities of drainage area and length, respectively [*Rodríguez-Iturbe and Rinaldo*, 1997; *Rigon et al.*, 1996; *Crave and Davy*, 1997; *Paik and Kumar*, 2011]. Different explanations of these power laws are available [*Banavar et al.*, 1999; *Dodds and Rothman*, 2000; *Birnir et al.*, 2001; *Banavar et al.*, 2001; *Birnir et al.*, 2007; *Birnir*, 2008; *Rinaldo et al.*, 2014], including self-organized dynamic systems [*Bak et al.*, 1988; *Rinaldo et al.*, 1993; *Marković and Gros*, 2014], invasion percolation [*Stark*, 1991] and minimum energy dissipation [*Rodríguez-Iturbe et al.*, 1992].

Catchment drainage networks are essentially static structures in the landscape, i.e., their temporal evolution cannot be readily measured. On the other hand, laboratory-based experimental geomorphology has a longstanding tradition [e.g., *Schumm and Khan*, 1971; *Flint*, 1973; *Mosley and Parker*, 1973; *Parker*, 1977] and permits detailed and rapid investigations of changes in surface morphology due to rainfall or overland flow [e.g., *Crave et al.*, 2000; *Brunton and Bryan*, 2000; *Römkens et al.*, 2002; *Hasbargen and Paola*, 2003; *Gómez et al.*, 2003; *Pelletier*, 2003; *Turowski et al.*, 2006; *Babault et al.*, 2007; *Yao et al.*, 2008; *Tatard et al.*, 2008; *Paola et al.*, 2009; *Bonnet*, 2009; *Berger et al.*, 2010; *Graveleau et al.*, 2012; *Rohais et al.*, 2012; *McGuire et al.*, 2013; *Reinhardt and Ellis*, 2015; *Sweeney et al.*, 2015]. For instance, dynamic changes of a rill network in uncohesive sediment under a constant uplift rate were observed by *Hasbargen and Paola* [2000]. In contrast, rill networks in a cohesive sediment evolved along the previously generated rills [*Bennett and Liu*, 2016] due to surface resistance. *Singh et al.* [2015] generated rill networks in a 0.5-m × 0.5-m experiment under spatially uniform but temporally variable rainfall and constant uplift rate. They found that the drainage area distribution was described by a power law with an exponent of 0.5. Similarly, *Bennett and Liu* [2016] examined rill formation at the flume scale (7 m × 2.4 m) and found an exponent of about 0.5 for Hack's law.

In summary, geometrical characteristics of catchment drainage networks have a high degree of similarity. These same characteristics are evident in channeled surfaces in laboratory studies. Here, we extend these studies by considering the flow network on an unchanneled sediment. Specifically, we measured the surface evolution of an unconsolidated sediment under non-uniform rainfall and overland flow such that no (observable) rills were formed.

However, the surface roughness produces a drainage network representation of the overland flow, which is then subjected to geometrical analysis.

2 Experiment

A 2-m × 1-m erosion flume with 5% slope (Figure S1) was filled to a depth of 15 cm with unconsolidated sediments that had a mean diameter of 0.53 mm (Table S1 and Figure S2, where S refers to the Supporting Information). Non-uniform rainfall with an average of 85 mm h^{-1} and Christiansen uniformity coefficient [*Christiansen*, 1942] of 26% was applied (Figure 1h). The non-uniform rainfall ensured that the flume drainage network varied both spatially and temporally due to non-uniform erosion of the initially planar surface. The flume had an impermeable base and was drained by a single, 4-cm wide outlet (Figure S1), located at ($x = 0$, $y = 0$). The sediment became fully saturated during the first 15 min of precipitation, which was accompanied by a rapid elevation drop at the outlet during the first 5 min. A 3D laser scanner, with about 4-mm resolution, was used to extract Digital Elevation Models (DEMs) at 0.25, 0.5, 1, 2, 4, 8 and 16 h. More details of the experimental setup are available in the Supporting Information. With the same design and precipitation distribution, another experiment was carried out at 10% slope with an average rainfall of 60 mm h^{-1} that lasted for 20 h. The results of this experiment, which are similar to those presented here, are included in the Supporting Information (Figures S8-S12).

3 Results and Discussion

The elevation change during the experiment is shown Figure 1. The sediment elevation was measured from the outlet ($z = 0$). For convenience, we refer to the ranges $z \leq 60$ mm and $z \geq 60$ mm as the downstream and upstream, respectively. Overall, the morphology evolution can be divided into two steps: (i) until $t = 4$ h, most of the variation occurred at the upstream end while the downstream end did not show any considerable evolution, and (ii) after $t = 4$ h, the downstream morphology propagates into the upstream.

To characterize the morphology, a network was generated based on the measured surface scans (Figure 1a-g) and precipitation (Figure 1h). Pit points were removed following *Planchon and Darboux* [2002]. Similarly to large scale river networks, the discharge distributions (Q) and drainage area (A) are computed via the D8 algorithm [*O'Callaghan and Mark*, 1984]:

$$Q_i = \sum_{j=1}^{8} w_{ji}\, Q_j + R_i\, \Delta x\, \Delta y \tag{1}$$

$$A_i = \sum_{j=1}^{8} w_{ji}\, A_j + \Delta x\, \Delta y \tag{2}$$

where the summation over j refers to the eight cells surrounding the ith cell. The slopes from each cell (i) into each of the eight neighbor cells (j) were calculated, with flow directed along the steepest descent. The value of w_{ji} is unity if the cell j flows into cell i, otherwise it is zero. R_i (mm h^{-1}) is rainfall intensity at cell i (Figure 1 h) and Δx (mm) and Δy (mm) are the grid sizes in x and y directions, respectively.

The distribution of drainage area and discharge at different times are plotted in Figures 2 and S4, respectively. At $t = 0.25$ h (Figure 2a), four separate branches depicted by A, B, C and D drained into the flume's outlet ($x = 0$, $y = 0$). Then, at $t = 0.5$ h (Figure 2b), branch C joined B and branch BC was generated while a minor change in the network was evident in the upper part of the network. After 1 h (Figure 2c), junction A became attached to BC and the pathway denoted ABC was formed. At $t = 2$ h (Figure 2d), the area drained by ABC inclined to the right side. Furthermore, branch D drained a greater proportion of the precipitation as it assumed part of the upstream area previously drained by ABC. Finally at $t = 4$ h, the

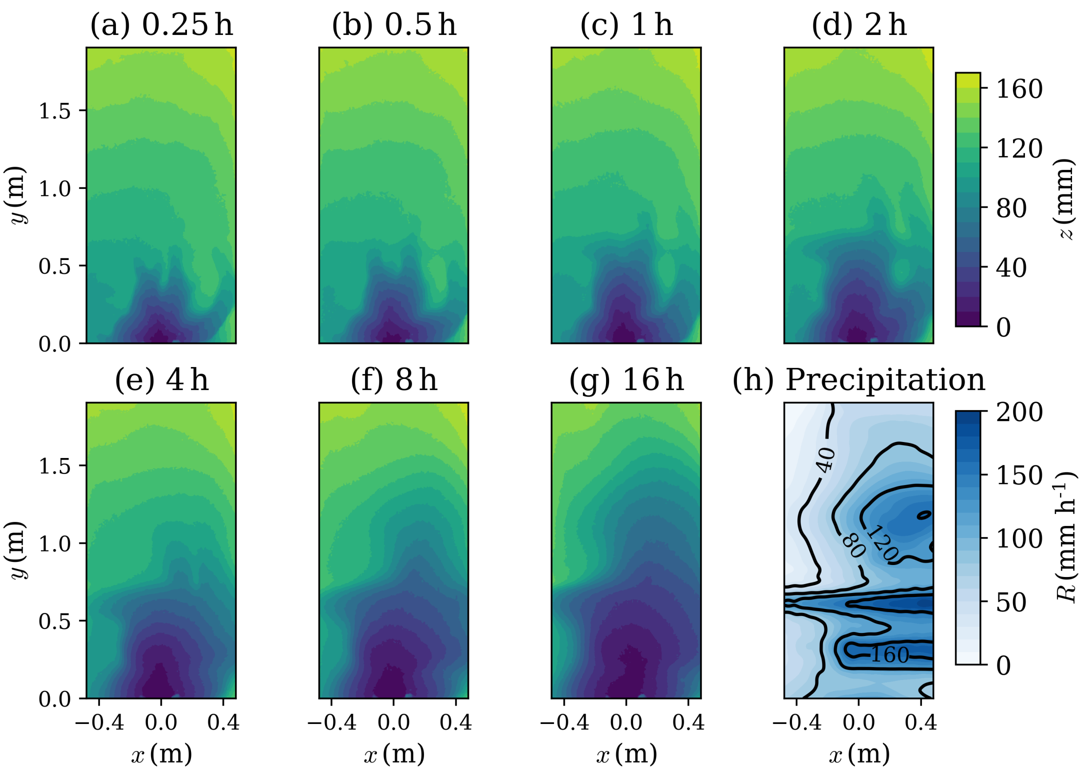

Figure 1. Measured morphology (z) evolution during the 16-h experiment (a-g). Initially, the flume slope was 5%, with $y = 0$ the lowest elevation and x being the transverse direction. The flume drained at a single point, located at $(x, y) = (0, 0)$. Due to the spatially non-uniform precipitation (h), the morphology changes increase from the left side (low precipitation rate area) towards the right (high precipitation rate area).

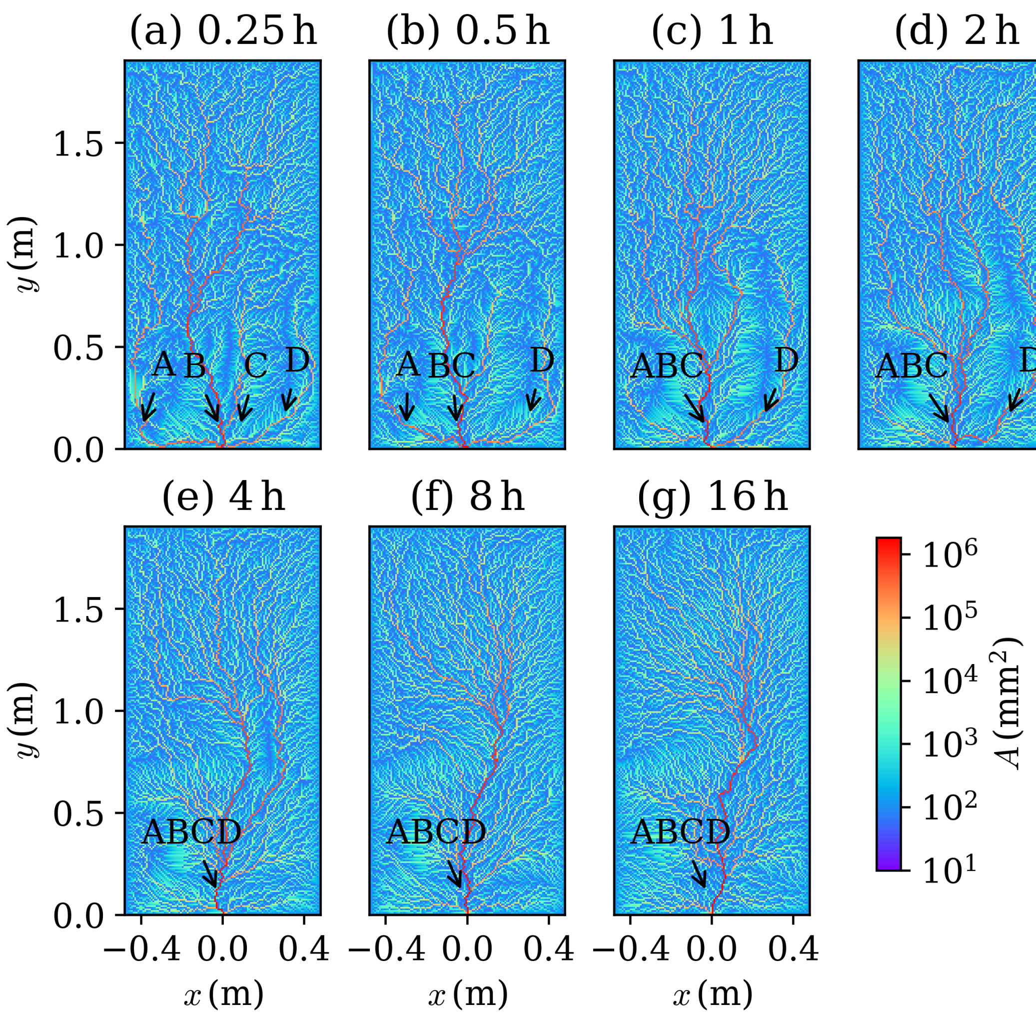

Figure 2. Drainage area (A) distribution determined using the D8 algorithm and the measured morphologies shown in Figure 1a-g. Initially, the flow paths, e.g., at t = 0.25 and 0.5 h, reflect the initial surface condition and central drainage point at the flume exit. The labels A-D identify the main drainage pathways, which coalesced with ongoing erosion over the course of the experiment. The impact of the higher-intensity rainfall on the right side of the flume is manifested in the main flow path, which moves to the right side during the experiment (more details given in the text).

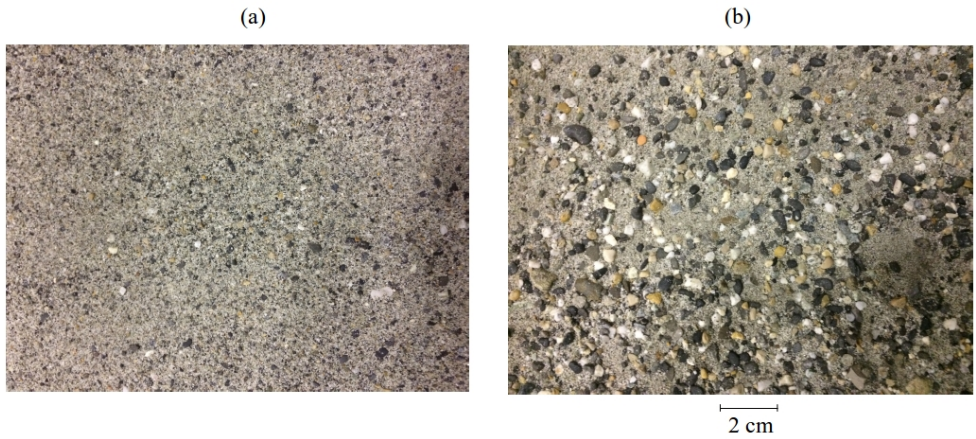

Figure 3. Sediment surface at $t = 0$ (a) and $t = 16$ h (b). The uncohesive sediment had a wide range of particle sizes. Smaller particles were preferentially eroded during the experiment, leaving the larger particles as shown in (b). The dynamics of this surface evolution are reflected in the changing drainage networks computed using the D8 algorithm (Figure 2).

network ABCD was generated (Figure 2e). At later times ($t = 8$ h and 16 h), the high flow part of ABCD became more dominant and moved to the right (Figure 2f and g). Variations in the drainage area network (and discharge network in Figure S4) mostly occurred in the first 8 h of the experiment, similarly to the surface morphology. Changes were less rapid in the second 8 h, although the main structure of the network was reinforced and some local changes to the low-order pathways took place. The evolution of the downstream (Figure 1e) started at the same time as the network (ABCD) was generated at $t = 4$ h (Figure 2e). The network's width function was computed for each scan to quantify its temporal evolution (Figure S5).

Even though the flow covers the entire surface and is continuous (except perhaps for raindrop impacts), the D8 algorithm leads to its description as a network, which was considerably reorganized during the 16-h rainfall duration (Figure 2). We recall that these networks do not represent observable surface rills, but rather the drainage network derived from the surface morphology as captured by the surface scans. As shown in Figure 3, due to shorter erosion time scales, the fine sediment particles are rapidly removed while the larger particles move slowly down the surface [*Hairsine and Rose*, 1992a,b; *Polyakov and Nearing*, 2003; *Sander et al.*, 2011; *Wang et al.*, 2014; *Kim and Ivanov*, 2014; *Cheraghi et al.*, 2016; *Lisle et al.*, 2017] or are not moved at all, resulting in a surface partially covered by motionless pebbles. Therefore, the network evolution is a result of size-dependent sediment particle transport and raindrop-driven rearrangement on the surface.

We next examine the statistical characteristics of the network. We first consider Hack's law [*Hack*, 1957], which is a well-known metric used in analyses of large scale river networks [*Maritan et al.*, 1996; *Rigon et al.*, 1996; *Dodds and Rothman*, 2001a]. For our case, the A-l distribution was divided into 20 bins on a logarithmic scale. For each bin, the ratio between consecutive average moments of length were calculated. The results are plotted in Figure 4 for the first to four moments of l ($n = 1, 2, 3, 4$). They show a validation of a finite-size scaling framework for the distributions of l, in the form of $p(l|A) = l^{-\xi} F(l/A^h)$ where $F(x) \to 0$ for $x \to \infty$ and $F(x) \to 0$ for $x \to 0$, analogous to large scale river networks [*Rigon et al.*, 1996]. The power-law relationship is maintained for at least two orders of magnitude, with the scaling exponent h in the range of [0.54-0.6]. Upper and lower cutoffs affecting the scaling range were expected. Lower cutoffs are basically the limits of detectability. Upper cutoffs are associated with the maximum cumulative area or flow rate [*Rigon et al.*,

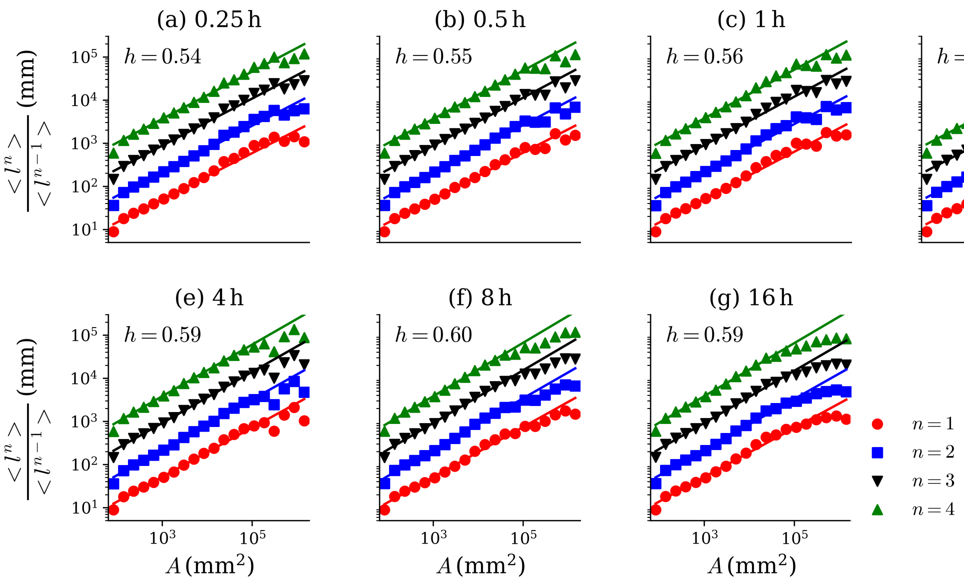

Figure 4. Ratios of consecutive moments of the upstream length distribution (l) at any point within subcatchments of area (A) identified by steepest descent directions. The slope of the log-log plot is Hack's exponent (h) at different times (t = 0.25-16 h). The A-l distribution was divided into 20 bins on a logarithmic scale, with the n^{th} moment of (l) for each bin denoted by $\langle l^n \rangle$. The curves of higher moments ($n > 1$) are shifted vertically for the purpose of visualization.

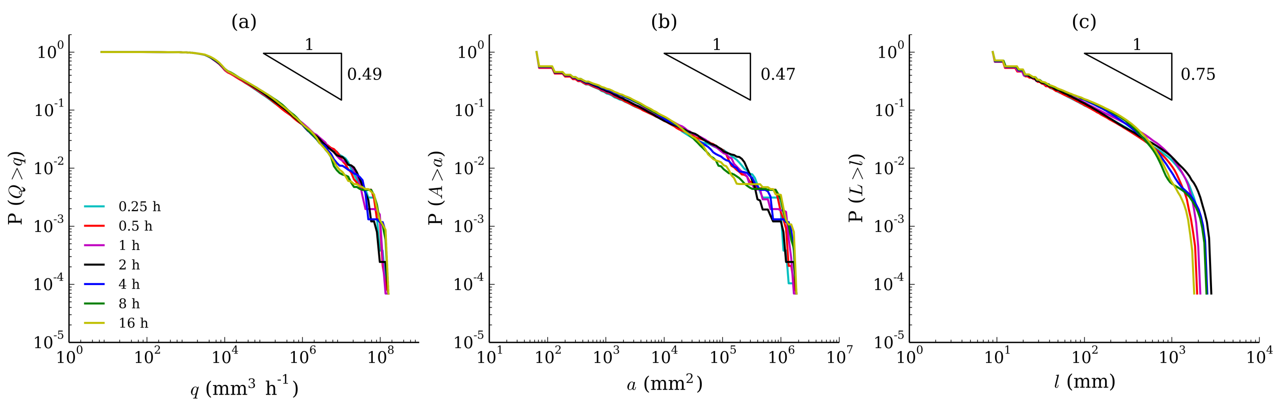

Figure 5. Plots (a)-(c) show, respectively, exceedance probabilities of discharge (Q), drainage area (A) and upstream length (l) at different times (t = 0.25-16 h)

1996]. Another experiment at 10% slope with an average rainfall of 60 mm h^{-1} (Figure S11) showed a range of [0.51-0.55] for the Hack exponent (h). For both experiments, the Hack exponents agree with those found for large scale river networks [*Hack*, 1957; *Gray*, 1961; *Mueller*, 1972; *Mosley and Parker*, 1973; *Mueller*, 1973; *Montgomery and Dietrich*, 1992; *Maritan et al.*, 1996; *Rigon et al.*, 1996, 1998], which are in the range [0.5-0.7], yet with a measured mean of about $h = 0.58$ [*Willemin*, 2000] and an analytical value of $h = 0.57$ [*Birnir*, 2008].

The distributions of (computed) drainage discharge, drainage area and upstream length are plotted in Figure 5. In Figure 5a, the flume discharge can be separated into low ($q \leq 1.1 \times 10^4$ mm h^{-1}), medium ($1.1 \times 10^4 < q < 3 \times 10^6$ mm h^{-1}) and high ($q \geq 3 \times 10^6$ mm h^{-1}) sections. The low discharge region mostly covers the left of the flume (Figure S4) where the precipitation rate is lower. The values of $P(Q > q)$ for these regions do not change during the network evolution (from 0.25 h to 16 h). For the medium discharge regions, a power-law relationship ($P(Q > q) = q^{-\varphi}$) describes the exceedance probability with an exponent of $\varphi = 0.49$. The high discharge area shows the most temporal variability, which corresponds to the changes of the main streams (A-D in Figure S4). Since the D8 algorithm selects a single adjacent down-gradient cell to receive water from a given cell, potentially the predicted flow becomes more localized than in reality. Also, flow disturbances due to raindrop impact and resulting mixing are not accounted for.

Due to spatial and temporal variations of precipitation in natural settings, the distribution of drainage area and upstream length are more commonly used metrics for describing river networks at large (spatial) scales. Even though in this study no rills formed, the distributions of drainage area and upstream length under this shallow, overland flow cross a number of scales characterized by power laws ($P(A > a) = a^{-\beta}$ and $P(L > l) = l^{-\psi}$) with $\beta = 0.47$ and $\psi = 0.75$, respectively (Figure 5b and c). Furthermore, at 10% slope with an average rainfall of 60 mm h^{-1}, exponents of 0.49, 0.47 and 0.71 were found for power laws describing discharge, drainage area and upstream length distributions, respectively (Figure S12). These results are similar to large scale river networks [*Mandelbrot*, 1977; *Tarboton et al.*, 1989; *Rigon et al.*, 1996; *Dodds and Rothman*, 2001a,b,c; *Rinaldo et al.*, 2014]. In addition, the values of these exponents are close to analytical results, $\beta = 1 - h$ and $\psi = \beta/h$, derived by *Maritan et al.* [1996].

The consistency between the laboratory results in Figs. 4 and 5, and results for catchment networks [e.g., *Rodríguez-Iturbe and Rinaldo*, 1997] points to an underlying governing principle operating at different scales, such as the principle of minimum energy expenditure [*Rodríguez-Iturbe et al.*, 1992] that applies at equilibrium conditions for river networks. Similarly, recent work (Smith 2018) on equilibrium landscapes showed that overland flows minimized a Lagrangian function of kinetic and potential energies. For both potential (viscosity dominated) and inviscid flows and for fixed boundary conditions, energy dissipation continues monotonically until the steady flow configuration is achieved, i.e., energy dissipation is a minimum [*Lord Rayleigh* , 1893]. The energy minimization principle has been shown exactly (by re-parametrization invariance arguments, and in the small gradient approximation) to correspond to the steady-state solution of the general landscape evolution equation in fluvial regions [*Banavar et al.*, 2001]. Deriving scaling properties and self-organization in optimal networks is therefore tantamount to analyzing the underlying equations if steady-state solutions are sought. Laboratory-scale rill networks were also shown to evolve towards the minimum energy expenditure [e.g., *Gómez et al.*, 2003; *Berger et al.*, 2010]. However, for unchanneled morphologies, further investigation is needed since our results suggest (approximately) time-invariant scaling laws for a rapidly eroding surface.

The dynamics of eroding surfaces and related overland flow (including raindrop impact) can be modeled via different approaches, from mechanistic models that consider coupled overland flow and soil erosion [e.g., *Nearing et al.*, 1989; *Hairsine and Rose*, 1992a,b] to catchment scale landscape evolution models (LEMs) [e.g., *Willgoose*, 1989; *Howard et al.*, 1994; *Perron et al.*, 2008; *Smith*, 2018]. LEMs, which predict channel networks at both the catchment and laboratory scales, are relevant to our experimental results. We emphasize that our experiment involves continuous overland flow on an unchanneled surface in contrast to channelized flow in a catchment. Nonetheless, characterization of the overland flow on the measured morphology via the D8 algorithm results in a network that is geometrically similar to a catchment drainage network. The D8 algorithm provides a network representation of the overland flow driven by gravity. This representation is an approximation, but allows for a direct comparison of the unchanneled surface morphology in our experiments with the channeled networks found in catchments and in laboratory experiments.

These experiments support a notable extension of what was previously thought about the kind of recursive features shown by channeled landscapes at much larger scales. Unchanneled landscapes were thought to obey diffusive evolution. For splash-dominated erosion studied here, the scaling structures were replicas of those occurring at orders of magnitude larger scales. It is totally remarkable that the aggregation patterns are independent of the specific sediment transport type in erosional patterns. Moreover, the temporal stability of the scaling structures we measure here suggests that indeed the planar features of steady states are reached almost immediately by erosional surfaces, as was speculated but never shown for real river networks. We suggest that the results could provide a test case for LEMs, which are applicable at both the laboratory [*Sweeney et al.*, 2015] and catchment scales [*Perron et al.*, 2009] on the condition that channels are formed. In the above-mentioned network analysis of *Banavar et al.* [2001], diffusion was ignored, although it is present in LEMs. Since diffusion effects will tend to smooth surfaces in LEM predictions, we speculate that our results will prompt additional investigations of the role of diffusion in these models. That is, it remains to be determined if the scale invariance uncovered in this work can be captured by LEMs.

4 Conclusions

An evolving unchanneled surface under a spatially non-uniform rainfall was statistically characterized in the same manner as large scale river networks by converting the continuous overland flow into drainage area and discharge networks. The measurements show that although the surface morphology and the corresponding overland flow network changed markedly during the experiment, the system preserved Hack's law and power laws in distributions of drainage area, length and discharge. More importantly, the exponents, the values of which are identical to large scale river networks, remained in a narrow range despite the considerable change in the surface morphology and the corresponding network structure. This work provides, for the first time, experimental support for the self-similar organization of landscapes even where observable rills or channels are not formed on the surface.

ACKNOWLEDGMENTS

Financial support was provided by the Swiss National Science Foundation (200021-144320). Seifeddine Jomaa, Antoine Wiedmer, Jacques Roland Golay, Pierre-Alain Hildenbrand, Htet Kyi Wynn and Julian A. Barry provided essential technical support for the execution of the experiment. We thank Sean J. Bennett and the two anonymous reviewers for their careful reviews which helped improve the manuscript. We also appreciate the collaboration of the SAGRAVE company, Lausanne, Switzerland. The surface morphology data are available at http://doi.org/10.5281/zenodo.1292113.

References

Babault, J., S. Bonnet, J. V. D. Driessche, and A. Crave (2007), High elevation of low-relief surfaces in mountain belts: Does it equate to post-orogenic surface uplift?, *Terra Nova*, *19*(4), 272–277, doi:10.1111/j.1365-3121.2007.00746.x.

Bak, P., C. Tang, and K. Wiesenfeld (1988), Self-organized criticality, *Physical Review A*, *38*(1), 364–374, doi:10.1103/PhysRevA.38.364.

Banavar, J. R., A. Maritan, and A. Rinaldo (1999), Size and form in efficient transportation networks, *Nature*, *399*, 130–132, doi:10.1038/20144.

Banavar, J. R., F. Colaiori, A. Flammini, A. Maritan, and A. Rinaldo (2001), Scaling, optimality, and landscape evolution, *Journal of Statistical Physics*, *104*(1-2), 1–48, doi:10.1023/A:1010397325029.

Bennett, S. J., and R. Liu (2016), Basin self-similarity, Hack's law, and the evolution of experimental rill networks, *Geology*, *44*(1), 35–38, doi:10.1130/G37214.1.

Berger, C., M. Schulze, D. Rieke-Zapp, and F. Schlunegger (2010), Rill development and soil erosion: A laboratory study of slope and rainfall intensity, *Earth Surface Processes and Landforms*, *35*(12), 1456–1467, doi:10.1002/esp.1989.

Birnir, B. (2008), Turbulent rivers, *Quarterly of Applied Mathematics*, *66*(3), 565–594, doi:10.1090/S0033-569X-08-01123-8.

Birnir, B., T. R. Smith, and G. E. Merchant (2001), The scaling of fluvial landscapes, *Computers and Geosciences*, *27*(10), 1189–1216, doi:10.1016/S0098-3004(01)00022-X.

Birnir, B., J. Hernandez, and T. R. Smith (2007), The stochastic theory of fluvial land surfaces, *Journal of Nonlinear Science*, *17*(1), 13–57, doi:10.1007/s00332-005-0688-3.

Bonnet, S. (2009), Shrinking and splitting of drainage basins in orogenic landscapes from the migration of the main drainage divide, *Nature Geoscience*, *2*(12), 897, doi:10.1038/ngeo700.

Brunton, D. A., and R. B. Bryan (2000), Rill network development and sediment budgets, *Earth Surface Processes and Landforms*, *25*(7), doi:10.1002/1096-9837(200007)25:7<783::AID-ESP106>3.0.CO;2-W.

Cheraghi, M., S. Jomaa, G. C. Sander, and D. A. Barry (2016), Hysteretic sediment fluxes in rainfall-driven soil erosion: Particle size effects, *Water Resources Research*, *52*(11), 8613–8629, doi:10.1002/2016WR019314.

Christiansen, J. E. (1942), Irrigation by sprinkling, California Agricultural Experiment Station Bulletin 670, Berkeley, https://archive.org/stream/irrigationbyspri670chri (last accessed 16 August 2018).

Crave, A., and P. Davy (1997), Scaling relationships of channel networks at large scales: Examples from two large-magnitude watersheds in Brittany, France, *Tectonophysics*, *269*(1-2), 91–111, doi:10.1016/S0040-1951(96)00142-4.

Crave, A., D. Lague, P. Davy, J. Kermarrec, D. Sokoutis, L. Bodet, and R. Compagnon (2000), Analogue modelling of relief dynamics, *Physics and Chemistry of the Earth, Part A: Solid Earth and Geodesy*, *25*(6), 549–553, doi:10.1016/S1464-1895(00)00084-3.

Dodds, P. S., and D. H. Rothman (2000), Scaling, universality, and geomorphology, *Annual Review of Earth and Planetary Sciences*, *28*(1), 571–610, doi:10.1146/annurev.earth.28.1.571.

Dodds, P. S., and D. H. Rothman (2001a), Geometry of river networks. I. Scaling, fluctuations, and deviations, *Physical Review E - Statistical Physics, Plasmas, Fluids, and Related Interdisciplinary Topics*, *63*(1), 016115, doi:10.1103/PhysRevE.63.016115.

Dodds, P. S., and D. H. Rothman (2001b), Geometry of river networks. II. Distributions of component size and number, *Physical Review E - Statistical Physics, Plasmas, Fluids, and Related Interdisciplinary Topics*, *63*(1), 016116, doi:10.1103/PhysRevE.63.016116.

Dodds, P. S., and D. H. Rothman (2001c), Geometry of river networks. III. Characterization of component connectivity, *Physical Review E*, *63*(1), 016117, doi:10.1103/PhysRevE.63.016117.

Flint, J.-J. (1973), Experimental development of headward growth of channel networks, *Geological Society of America Bulletin*, *84*(3), 1087–1094, doi:10.1130/0016-7606(1973)84<1087:EDOHGO>2.0.CO;2.

Gómez, J. A., F. Darboux, and M. A. Nearing (2003), Development and evolution of rill networks under simulated rainfall, *Water Resources Research*, *39*(6), 1148, doi:10.1029/2002WR001437.

Graveleau, F., J. Malavieille, and S. Dominguez (2012), Experimental modelling of orogenic wedges: A review, *Tectonophysics*, *538*, 1–66, doi:10.1016/j.tecto.2012.01.027.

Gray, D. M. (1961), Interrelationships of watershed characteristics, *Journal of Geophysical Research*, *66*(4), 1215–1223, doi:10.1029/JZ066i004p01215.

Hack, J. T. (1957), *Studies of Longitudinal Stream Profiles in Virginia and Maryland*, vol. 294, US Government Printing Office, https://pubs.er.usgs.gov/publication/pp294B (last accessed 16 August 2018).

Hairsine, P. B., and C. W. Rose (1992a), Modeling water erosion due to overland flow using physical principles: 1. Sheet flow, *Water Resources Research*, *28*(1), 237–243, doi:10.1029/91WR02380.

Hairsine, P. B., and C. W. Rose (1992b), Modeling water erosion due to overland flow using physical principles: 2. Rill flow, *Water Resources Research*, *28*(1), 245–250, doi:10.1029/91WR02381.

Hasbargen, L. E., and C. Paola (2000), Landscape instability in an experimental drainage basin, *Geology*, *28*(12), 1067–1070, doi:10.1130/0091-7613(2000)28<1067:LIIAED>2.0.CO.

Hasbargen, L. E., and C. Paola (2003), How predictable is local erosion rate in eroding landscapes?, *Prediction in Geomorphology*, pp. 231–240, doi:10.1029/135GM16.

Howard, A., W. Dietrich, and M. A. Seidl (1994), Modeling fluvial erosion on regional to continental scales, *Journal of Geophysical Research*, *99*, 13,971–1398, doi:10.1029/94JB00744.

Kim, J., and V. Y. Ivanov (2014), On the nonuniqueness of sediment yield at the catchment scale: The effects of soil antecedent conditions and surface shield, *Water Resources Research*, *50*(2), 1025–1045, doi:10.1002/2013WR014580.

Lisle, I. G., G. C. Sander, J.-Y. Parlange, C. W. Rose, W. L. Hogarth, R. D. Braddock, F. Stagnitti, D. A. Lockington, S. Jomaa, M. Cheraghi, and D. A. Barry (2017), Transport time scales in soil erosion modeling, *Vadose Zone Journal*, *16*(12), doi:10.2136/vzj2017.06.0121.

Lord Rayleigh (1893), On the flow of viscous liquids, especially in two dimensions, *The London, Edinburgh, and Dublin Philosophical Magazine and Journal of Science*, *36*(221), 354–372, doi:10.1080/14786449308620489.

Mandelbrot, B. B. (1977), *The Fractal Geometry of Nature*, W. H. Freeman and Company, New York, USA.

Maritan, A., A. Rinaldo, R. Rigon, A. Giacometti, and I. Rodríguez-Iturbe (1996), Scaling laws for river networks, *Physical Review E*, *53*, 1510–1515, doi:10.1103/PhysRevE.53.1510.

Marković, D., and C. Gros (2014), Power laws and self-organized criticality in theory and nature, *Physics Reports*, *536*(2), 41–74, doi:10.1016/j.physrep.2013.11.002.

McGuire, L. A., J. D. Pelletier, J. A. Gómez, and M. A. Nearing (2013), Controls on the spacing and geometry of rill networks on hillslopes: Rain splash detachment, initial hillslope roughness, and the competition between fluvial and colluvial transport, *Journal of Geophysical Research: Earth Surface*, *118*(1), 241–256, doi:10.1002/jgrf.20028.

Montgomery, D. R., and W. E. Dietrich (1992), Channel initiation and the problem of landscape scale, *Science*, *255*(5046), 826–830, doi:10.1126/science.255.5046.826.

Mosley, M. P., and R. S. Parker (1973), Re-evaluation of the relationship of master streams and drainage basins: Discussion, *Geological Society of America Bulletin*, *84*(9), 3123, doi:10.1130/0016-7606(1973)84<3123:ROTROM>2.0.CO;2.

Mueller, J. E. (1972), Re-evaluation of the relationship of master streams and drainage basins, *Bulletin of the Geological Society of America*, *83*(11), 3471–3474, doi:10.1130/0016-7606(1972)83[3471:ROTROM]2.0.CO;2.

Mueller, J. E. (1973), Re-evaluation of the relationship of master streams and drainage basins: Reply, *Geophysical Society of America Bulletin*, *84*(9), doi:10.1130/0016-7606(1973)84<3127:ROTROM>2.0.CO;2.

Nearing, M. A., G. R. Foster, L. J. Lane, and S. C. Finkner (1989), A process-based soil erosion model for USDA-water erosion prediction project technology, *Transactions of the ASAE*, *32*(5), 1587, doi:10.13031/2013.31195.

O'Callaghan, J. F., and D. M. Mark (1984), The extraction of drainage networks from digital elevation data, *Computer Vision, Graphics, and Image Processing*, *28*(3), 323–344, doi:10.1016/S0734-189X(84)80011-0.

Paik, K., and P. Kumar (2011), Power-law behavior in geometric characteristics of full binary trees, *Journal of Statistical Physics*, *142*(4), 862–878, doi:10.1007/s10955-011-0125-y.

Paola, C., K. Straub, D. Mohrig, and L. Reinhardt (2009), The “unreasonable effectiveness” of stratigraphic and geomorphic experiments, *Earth-Science Reviews*, *97*(1-4), 1–43, doi:10.1016/j.earscirev.2009.05.003.

Parker, R. S. (1977), Experimental study of drainage basin evolution and its hydrologic implications, PhD Thesis, Colorado State University, Fort Collins, Colorado, USA.

Pelletier, J. D. (2003), Drainage basin evolution in the Rainfall Erosion Facility: Dependence on initial conditions, *Geomorphology*, *53*(1), 183–196, doi:10.1016/S0169-555X(02)00353-7.

Perron, J. T., W. E. Dietrich, and J. W. Kirchner (2008), Controls on the spacing of first-order valleys, *Journal of Geophysical Research: Earth Surface*, *113*(4), 1–21, doi:10.1029/2007JF000977.

Perron, J. T., J. W. Kirchner, and W. E. Dietrich (2009), Formation of evenly spaced ridges and valleys, *Nature*, *460*(7254), 502–505, doi:10.1038/nature08174.

Planchon, O., and F. Darboux (2002), A fast, simple and versatile algorithm to fill the depressions of digital elevation models, *CATENA*, *46*(2), 159–176, doi:10.1016/S0341-8162(01)00164-3.

Polyakov, V. O., and M. A. Nearing (2003), Sediment transport in rill flow under deposition and detachment conditions, *CATENA*, *51*(1), 33–43, doi:10.1016/S0341-8162(02)00090-5.

Reinhardt, L., and M. A. Ellis (2015), The emergence of topographic steady state in a perpetually dynamic self-organized critical landscape, *Water Resources Research*, *51*(7), 4986–5003, doi:10.1002/2014WR016223.

Rigon, R., I. Rodríguez-Iturbe, A. Maritan, A. Giacometti, D. G. Tarboton, and A. Rinaldo (1996), On Hack’s law, *Water Resources Research*, *32*(11), 3367–3374, doi:10.1029/96WR02397.

Rigon, R., I. Rodríguez-Iturbe, and A. Rinaldo (1998), Feasible optimality implies Hack’s law, *Water Resources Research*, *34*(11), 3181–3189, doi:10.1029/98WR02287.

Rinaldo, A., I. Rodríguez-Iturbe, R. Rigon, E. Ijjasz-Vasquez, and R. L. Bras (1993), Self-organized fractal river networks, *Physical Review Letters*, *70*(6), 822–825, doi:10.1103/PhysRevLett.70.822.

Rinaldo, A., R. Rigon, J. R. Banavar, A. Maritan, and I. Rodríguez-Iturbe (2014), Evolution and selection of river networks: statics, dynamics, and complexity, *Proceedings of the National Academy of Sciences of the United States of America*, *111*(7), 2417–24, doi:10.1073/pnas.1322700111.

Rodríguez-Iturbe, I., and A. Rinaldo (1997), *Fractal River Basins: Chance and Self-Organization*, Cambridge University Press, Cambridge, UK.

Rodríguez-Iturbe, I., A. Rinaldo, R. Rigon, R. L. Bras, E. Ijjasz-Vasquez, and A. Marani (1992), Fractal structures as least energy patterns: The case of river networks, *Geophysical Research Letters*, *19*(9), 889–892, doi:10.1029/92GL00938.

Rohais, S., S. Bonnet, and R. Eschard (2012), Sedimentary record of tectonic and climatic erosional perturbations in an experimental coupled catchment-fan system, *Basin Research*, *24*(2), 198–212, doi:10.1111/j.1365-2117.2011.00520.x.

Römkens, M. J. M., K. Helming, and S. N. Prasad (2002), Soil erosion under different rainfall intensities, surface roughness, and soil water regimes, *CATENA*, *46*(2), 103–123, doi:10.1016/S0341-8162(01)00161-8.

Sander, G. C., T. Zheng, P. Heng, Y. Zhong, and D. A. Barry (2011), Sustainable soil and water resources: Modelling soil erosion and its impact on the environment, in *19th International Congress on Modelling and Simulation*, pp. 45–56, Modelling and Simulation Society of Australia and New Zealand Inc., Perth, Australia, http://mssanz.org.au/modsim2011/plenary.htm (last accessed 16 August 2018).

Schumm, S. A., and H. R. Khan (1971), Experimental study of channel patterns, *Nature*, *233*(5319), 407–409, doi:10.1038/233407a0.

Singh, A., L. Reinhardt, and E. Foufoula-Georgiou (2015), Landscape reorganization under changing climatic forcing: Results from an experimental landscape, *Water Resources Research*, *51*(6), 4320–4337, doi:10.1002/2015WR017161.

Smith, T. R. (2018), Analytic theory of equilibrium fluvial landscapes: The integration of hillslopes and channels, *Journal of Geophysical Research: Earth Surface*, *123*(3), 557–615, doi:10.1002/2016JF004073.

Stark, C. P. (1991), An invasion percolation model of drainage network evolution, *Nature*, *352*(6334), 423–425, doi:10.1038/352423a0.

Sweeney, K. E., J. J. Roering, and C. Ellis (2015), Experimental evidence for hillslope control of landscape scale, *Science*, *349*(6243), 51–53, doi:10.1126/science.aab0017.

Tarboton, D. G., R. L. Bras, and I. Rodríguez-Iturbe (1989), Scaling and elevation in river networks, *Water Resources Research*, *25*(9), 2037–2051, doi:10.1029/WR025i009p02037.

Tatard, L., O. Planchon, J. Wainwright, G. Nord, D. Favis Mortlock, N. Silvera, O. Ribolzi, M. Esteves, and C. H. Huang (2008), Measurement and modelling of high-resolution flow-velocity data under simulated rainfall on a low-slope sandy soil, *Journal of Hydrology*, *348*(1-2), 1–12, doi:10.1016/j.jhydrol.2007.07.016.

Turowski, J. M., D. Lague, A. Crave, and N. Hovius (2006), Experimental channel response to tectonic uplift, *Journal of Geophysical Research: Earth Surface*, *111*(F3), F03008, doi:10.1029/2005JF000306.

Wang, L., Z. Shi, J. Wang, N. Fang, G. Wu, and H. Zhang (2014), Rainfall kinetic energy controlling erosion processes and sediment sorting on steep hillslopes: A case study of clay loam soil from the Loess Plateau, China, *Journal of Hydrology*, *512*, 168–176, doi:10.1016/j.jhydrol.2014.02.066.

Willemin, J. H. (2000), Hack's Law: Sinuosity, convexity, elongation, *Water Resources Research*, *36*(11), 3365–3374, doi:10.1029/2000WR900229.

Willgoose, G. R. (1989), A physically based channel network and catchment evolution model, PhD Thesis, Massachusetts Institute of Technology, Massachusetts Institute of Technology, Dept. of Civil Engineering, Massachusetts, USA.

Yao, C., T. Lei, W. J. Elliot, D. K. McCool, J. Zhao, and S. Chen (2008), Critical conditions for rill initiation, *Transactions of the ASABE*, *51*(1), 107–114, doi:10.13031/2013.24231.